Supporting information:

Wavelength-Dependent Laser-Induced Dynamic Nano-Annealing of Single Plasmonic Antennas

*Shuang Zhou†, Zhong Wang†, Chenyu Dong, Jie Bian and Weihua Zhang**

College of Engineering and Applied Sciences, Jiangsu Key Laboratory of Artificial Functional Materials, MOE Key Laboratory of Intelligent Optical Sensing and Manipulation, State Key Laboratory of Analytical Chemistry for Life Sciences, Nanjing University, Nanjing 210093, China

* Corresponding author: zwh@nju.edu.cn

† These authors contributed equally to this work

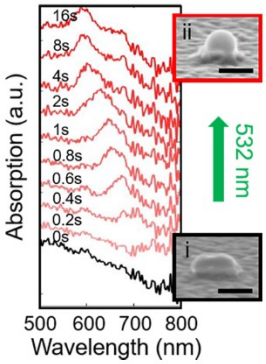

Figure S1 Continuous absorption spectral change of a VCCPA in a laser annealing process at 532 nm. The insets are corresponding SEM images of the antenna before (black solid line) and after (red solid line) being annealed. The resonance appears after being annealed for just 0.2 seconds, and it continuously blue shifts for about 150 nm under the 532 nm laser irradiation (the laser power is < 20 mW). Scale bar: 100 nm.

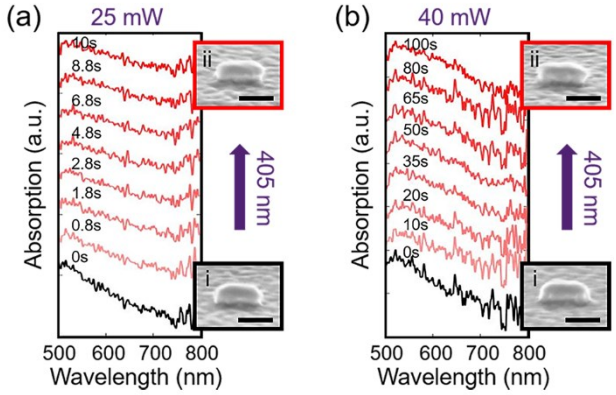

Figure S2 Absorption spectra of a VCCPA in the annealing process at 405 nm with the laser power below 50 mW. The applied laser powers are 25 mW in (a) and 40 mW in (b). No spectral change was observed. Scale bar: 100 nm.

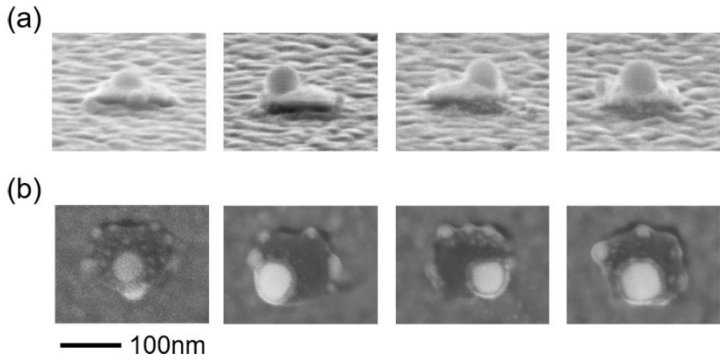

Figure S3 The melted nanospheres at different positions on the Si nanopillars. (a) Grazing incidence SEM images of the structures after being annealed by 532 nm laser. (b) Corresponding top-view SEM images of the corresponding structures after being annealed by 532 nm laser.

Simulation model in Comsol Multiphysics

To obtain the temperature distribution of the single VCCPA structure irradiated by 532 nm and 405 nm laser, we built a simulation model using Comsol Multiphysics. The simulation consists of two steps: (i) using "Electromagnetic Wave, Frequency Domain" module to calculate the field distribution and get the heat generation, and (ii) coupling "Heat Transfer in Solids" module to obtain the temperature distribution. As shown in Fig. S4, we define two calculation regions, the red box (500 nm × 500 nm × 500 nm) and the black box (2 μm × 2 μm × 2 μm) for the two steps respectively. In the first step, the field intensity of the incident plane wave is set to be 6×10^6 V/m corresponding to a laser power of 20 mW and a laser spot size of 800 nm. For comparison, we use the same setting of the incident field in both 532 nm and 405 nm simulation. The heat generation can be written

as $Q = 1/2 \cdot Re(\boldsymbol{J} \cdot \boldsymbol{E}^*)$, and is set as the electromagnetic heat source in the second step. And the temperature distribution can be get from the heat conduction equation: $\rho C_P \cdot \frac{\partial T}{\partial t} = \nabla \cdot (k \nabla T) + Q$. We also calculated temperature of the gold nanostructure with different initial settings (laser power) at 532 nm. As shown in Fig. S5, the temperature increases linearly with laser power.

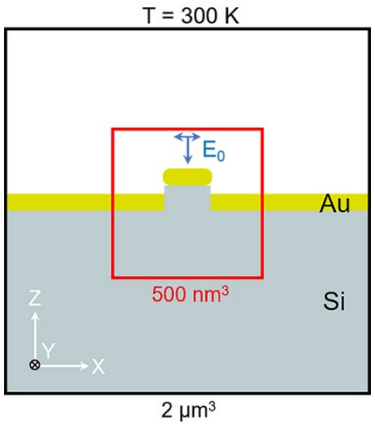

Figure S4 Schematic illustration of the simulation model in Comsol Multiphysics.

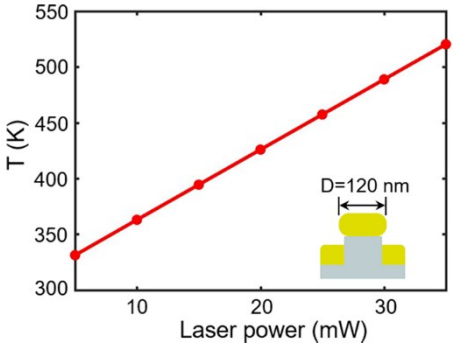

Figure S5 Simulated temperature of the gold nanostructure as the function of the laser power.

Conductivity measurement as direct proof for annealing-induced gap opening.

To check the change of the connection between the Au nanodisk and Au backplane, we measured the I-V curve of a single nanoantenna before and after being annealed using a conductive AFM. Here, VCCPAs on a polymer substrate were used instead of the Si substrate to make sure that the electrical conduction is solely related to the Au atoms in the nanogap. In measurements, we first grounded the Au backplane, and then determined the position of the VCCPA antennas by scanning the sample's morphology. After that, we ramped up the voltage of the tip, and the connectivity of the antenna can be directly characterized by measuring the currents through the tip.

In the case of un-heated antenna, there were a large amount of Au adatoms deposited in the nanogap, causing the connection between the Au nanodisk and backplane. As a results, The circuit was electrically conductive, and the current changed abruptly around 0 V when the voltage increases from - 0.5 V to 0.5 V. On the contrary, in the case of annealed antenna, the current stayed at zero because the Au nanodisk was separated from backplane.

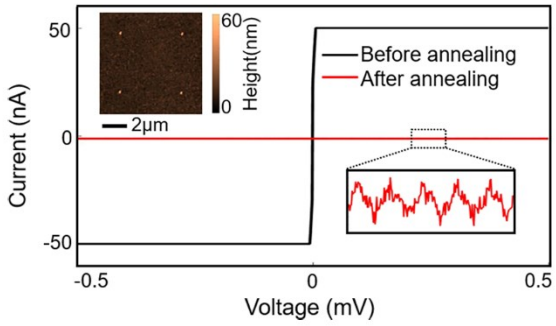

Figure S6 I - V curves of the same VCCPA structure before and after being annealed on a hot plate. The inset shows the AFM profile of the sample.

Simulated absorption spectrum

The simulation was done under normal illumination of linearly polarized light. The electric field is along the Au nanodisk in the plane of screen.

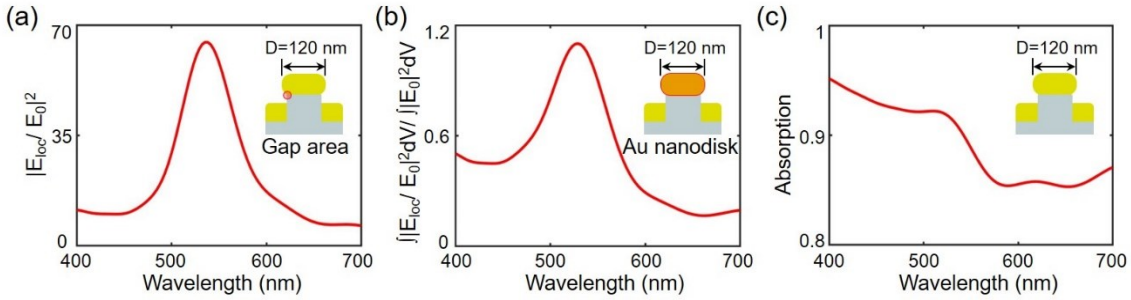

Figure S7 (a) Simulated enhancement spectrum of the local light intensity at the edge of Au nanodisk (the observation spot is marked with a red circle and the size of the nanodisk is 120 nm). (b) Simulated average enhancement spectrum of the light intensity over the whole cross-section of the Au nanodisk. (c) Simulated absorption spectrum of the whole plasmonic nanostructure (incl. Au nanodisk, Au backplane, Si pillar and Si substrate).

Absorption spectrum in the full spectral range (400 nm – 800 nm).

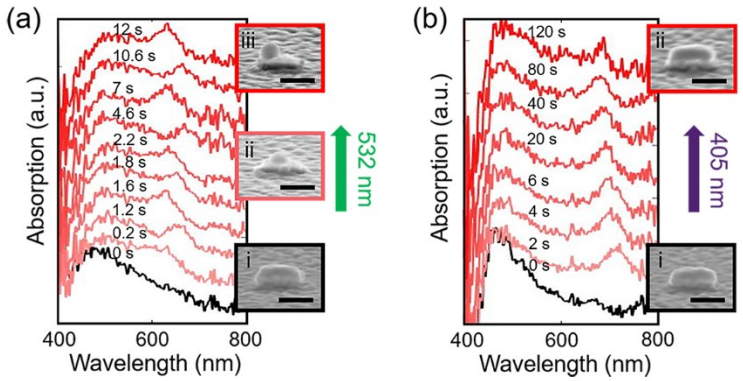

Figure S8 Absorption spectra starting from the 400 nm of a VCCPA in a laser annealing process at 532 nm (a) and 405 nm (b). The insets are corresponding SEM images of the antenna before (black solid line) and after (red solid line) being annealed. The abrupt

attenuation of the absorption in all the spectra is due to the limitation of the light source in our experiment. The light intensity is very weak below about 450 nm. However, it doesn't matter because the plasmonic response of Au nanoantenna is above 500 nm. Scale bar: 100 nm.

Time-share fashion measurement.

The white light spectrum measurement and the laser annealing process were done in a time-share fashion to avoid the interference of the annealing laser to the spectral measurements. We placed two shutters, shutter 1 and shutter 2 in front of the annealing laser and spectrometer, respectively. In measurements, shutter 1 was first open for *t1* to anneal the sample, then it was closed for *t2*, and the reflection spectra of the sample were collected. This process was repeated automatically with a homemade software by Labview, which also shows the absorption spectra in real-time and allows us to adjust parameters, such as the exposure time (*t1*), collection time (*t2*) and number of annealing cycles. Typically, a single annealing period, *t1*, was 0.2 s, the spectrum collection time, *t2*, was 2 s, and the cycle number was between 50 to 1000.

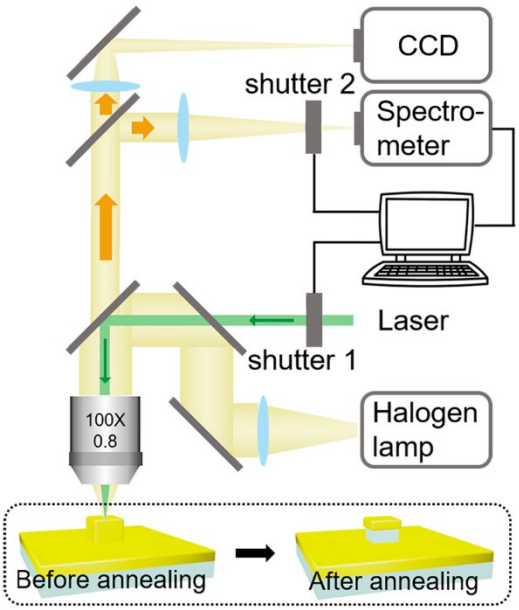

Figure S9 Sketch of the experimental setup.